

# Angstrom-resolution single-molecule fluorescence resonance energy transfer reveals mechanisms of DNA helicases

Wenxia Lin<sup>1</sup>, Jianbing Ma<sup>1</sup>, Dagan Nong<sup>1</sup>, Chunhua Xu<sup>1</sup>, Bo Zhang<sup>2</sup>, Jinghua

Li<sup>1</sup>, Qi Jia<sup>1</sup>, Shuoxing Dou<sup>1,4</sup>, Xuguang Xi<sup>2,3</sup>, Ying Lu<sup>1,\*</sup> and Ming Li<sup>1,4†</sup>

<sup>1</sup>*Beijing National Laboratory for Condensed Matter Physics and CAS Key Laboratory of Soft Matter Physics, Institute of Physics, Chinese Academy of Sciences, Beijing 100190, China.*

<sup>2</sup>*College of Life Sciences, Northwest A & F University, Yangling, Shaanxi 712100, China.*

<sup>3</sup>*LBPA, ENS de Cachan, CNRS, Universit Paris-Saclay, F-94235 Cachan, France.*

<sup>4</sup>*School of Physical Sciences, University of Chinese Academy of Sciences, Beijing 100049, China.*

(Dated: September 4, 2021)

Single-molecule FRET is widely used to study helicases by detecting distance changes between a fluorescent donor and an acceptor anchored to overhangs of a forked DNA duplex. However, it has lacked single-base pair (1-bp) resolution required for revealing stepping dynamics in unwinding because FRET signals are usually blurred by thermal fluctuations of the overhangs. We designed a nanotensioner in which a short DNA is bent to exert a force on the overhangs, just as in optical/magnetic tweezers. The strategy improved the resolution of FRET to 0.5 bp, high enough to uncover the differences in DNA unwinding by yeast Pif1 and *E. coli* RecQ whose unwinding behaviors cannot be differentiated by currently practiced methods. We found that Pif1 exhibits 1-bp-stepping kinetics, while RecQ breaks 1 bp at a time but sequesters the nascent nucleotides and releases them randomly. The high-resolution data allowed us to propose a three-parameter model to quantitatively interpret the apparently different unwinding behaviors of the two helicases which belong to two superfamilies.

Helicases are motor proteins involved in almost every aspect of nucleic acid metabolism [1–4]. When a helicase is loaded onto one of the overhangs (i.e., the tracking strand) of a forked DNA duplex and unwinds it, two nucleotides would be released per base pair unwound, leading to an increase in end-to-end distance of the overhangs. It is of great interest to know how a helicase uses the discrete energy derived from NTP hydrolysis to unwind DNA. The question remained unanswered for most helicases due to the lack of proper methods that can interrogate the stepping kinetics of helicases [5–7]. Optical tweezers (OT) are so far the most reliable technique to study single helicases with 0.5-bp resolution [8–10]. However, high-resolution measurements with OT require complicated instrumentation that is accessible to few laboratories only. In addition, OT measures one molecule at a time so that the throughput is usually very low. smFRET is a high-throughput technique for helicase assays. Using wide-field fluorescence microscopy, one can routinely record signals in parallel from hundreds of single molecules tethered to a surface [11–14]. To date,

the resolution of smFRET is limited to 2-3 bp when forked DNA is used as the substrate because of the softness of the single-stranded overhangs (Figure 1a). If a tension is exerted on the overhangs to suppress the fluctuations, the distance between the two fluorophores can be both stabilized and increased and the resolution of smFRET would thus be improved. The idea has led to the combination of optical or magnetic tweezers with smFRET in a few single-molecule studies [15–19]. These experiments, however, are even more difficult to perform because the fluorophores are prone to bleach during operations with the tweezers.

In the present work, by mimicking the tweezer-enhanced smFRET, we designed a nanotensioner with which a short DNA duplex is bent to stretch the two overhangs of the forked DNA (Figure 1b). Due to mismatch of their lengths, the short DNA duplex is bent to an arc, exerting a force on the fork. The force depends on the DNA construction. It is about 6 pN in one of our designs and the FRET change induced by each base pair unwound is about 0.13 (Figure 1), which is large enough to be readily recorded by many commercial single-molecule fluorescence microscopes. In contrast, the value is only about 0.04 when a forked DNA with free overhangs is used (Figure 1a). We applied the nanotensioner method to assess two helicases, namely, the yeast Pif1 and the *E. coli* RecQ. Pif1 is a prototypical member of the 5' -3' directed helicase superfamily 1B that is conserved from yeast to human [20–22]. It plays critical roles in the maintenance of telomeric DNA via catalytic inhibition of telomerase [23–26]. RecQ is a member of superfamily 2 helicases [27, 28]. It translocates in the 3' to 5' direction and contains the conserved DEAH box motif [29]. RecQ plays an important role in DNA damage response, chromosomal stability maintenance and has a vital role in maintaining genome homeostasis [30–33]. We did not observe significant differences between the unwinding behaviors of the two helicases with the forked DNA substrates as in conventional FRET assays. With the nanotensioner, however, the difference became obvious, enabling us to interrogate the molecular mechanisms of the two helicases with unprecedentedly deep insight.

The design of the nanotensioner (Figure 1b) is based on the fact that dsDNA is semi-flexible [34] with a bending modulus of  $B \approx 200 \text{ pN} \times \text{nm}^2$ . When a short dsDNA with a contour length  $S$  is bent to an arc of radius  $R$ , the bending energy is  $W = BS/2R^2$ . An ssDNA string of length  $x = 2R \sin(S/2R)$  maintains the radius of the dsDNA arc by exerting a force  $F$  on the two ends of the dsDNA segment. The force can be calculated according to  $F = -\delta W/\delta x$ , which reads as [35]

$$F = \frac{BS}{R^3} \left[ 2 \sin\left(\frac{S}{2R}\right) - \frac{S}{R} \cos\left(\frac{S}{2R}\right) \right]^{-1}. \quad (1)$$

It is also the tension exerted on the ssDNA overhangs of the forked DNA to be unwound. We attached a pair of dyes (Cy3 and Cy5) near the junction between the ssDNA overhangs and the duplex of the forked dsDNA. It is worth noting that, to serve our purpose of studying the unwinding stepping kinetics of a helicase, the DNA construct should meet the following conditions: (i) The tension on the string should be strong enough so that the change in FRET induced by one base pair unwound is not smaller than 0.1, which is the value required to recognize a step by our instrument; (ii) The tension does not decrease too much upon duplex unwinding so that the steps are basically uniform during the experiments.

Our calculations indicated that the DNA construct in Figure 1b will meet the above conditions and work well when the initial length of the string is in the range from 15 to 40 nt and the length of the dsDNA arc ranges from 50 to 100 bp. Shown in Figure 1c is the calculated FRET efficiency versus number of base pairs unwound for three typical

nanotensioners. The average FRET change is about 0.13 as 1 bp is unwound, which is large enough to be resolved by our instrument. The tension decreases slightly when the string length increases due to the newly added nucleotides (Figure 1d). In the present work, we used a DNA nanotensioner with a 60-bp dsDNA arc and a 30-nt ssDNA string. The DNA duplex to be unwound had a length of 40 bp, of which only 15 bp from the junction would be effective in the smFRET assay because of the limited measurement range of FRET ( $<10$  nm).

In order to show advantages of FRET with nanotensioners, we first characterized the unwinding kinetics with a forked DNA substrate as in conventional FRET assays (Figure 1a). The experiments were performed with objective-based total-internal-reflection fluorescence microscopy in imaging buffer composed of 25 mM Tris-HCl (pH 7.5), 50 mM NaCl, 5 mM MgCl<sub>2</sub>, 2 mM DTT and an oxygen scavenging system (0.8% D-glucose; 1 mg/ml glucose oxidase; 0.4 mg/ml catalase; 1 mM Trolox). Similar unwinding bursts were observed for the both helicases in buffers containing 5 nM helicase and 20  $\mu$ M ATP. Because the DNA unwinding rate can be regulated by ATP concentration, we reduced the ATP concentration to 0.5-2  $\mu$ M in order to see possible unwinding steps [12, 13]. Unfortunately, it was not easy to identify stepping events for either Pif1 or RecQ. The results indicated that thermal fluctuations of the displaced ssDNA indeed blur the FRET signals. Moreover, the fluctuations make it hard to convert the FRET changes to step sizes unambiguously.

We repeated the experiments to show the feasibility of the nanotensioner method. We observed distinct unwinding steps when the ATP concentration was reduced to 1  $\mu$ M (Figure 2a). The corresponding FRET values are in agreement with the theoretical calculations assuming that Pif1 unwinds 1 bp at a time. We built a histogram of the steps (Figure 2b) in the FRET range from 0.2 to 0.8 in which an approximately linear relationship exists between the distance of the two dyes and the observed FRET value [36, 37]. The distribution is narrow and has a peak at  $\Delta FRET = 0.14 \pm 0.02$ . The measurements at 0.5  $\mu$ M ATP yielded similar results. We also built histograms of dwell times before each stepping event (Figure 2c). Nonlinear least-squares analyses indicate that these distributions are best described by a single-exponential function, suggesting that these dwells are governed by a single kinetic event. It is an expected behavior for binding of a single ATP molecule before each step under limiting ATP concentrations. The decay time ( $0.32 \pm 0.08$  s) at 1  $\mu$ M ATP is about half of that ( $0.58 \pm 0.06$  s) at 0.5  $\mu$ M ATP, suggesting that the dwell is dominated by the time the protein takes to bind a single ATP. All together, these results are consistent with a model in which the enzyme hydrolyses a single ATP at a time and unzips the duplex with a uniform step size of 1 bp.

In contrast to the results for Pif1 in Figure 2, the unwinding steps of RecQ are not uniform even with the nanotensioner substrate. Shown in Figure 3 are representative unwinding bursts of RecQ recorded at low ATP concentrations. We observed events in which the DNA overhangs increased in length with various increments. The distributions of the increments, i.e., the step sizes, are composed of multiple peaks. Beside the expected peak corresponding to unwinding of 1 bp, the distribution at 2  $\mu$ M ATP shows other peaks corresponding to unwinding of 0.5, 1.5, 2.0, 2.5 and 3.0 bp, respectively. Similarly, the distribution of step sizes at 5  $\mu$ M ATP also shows a few major peaks, centered at 1.0, 1.5, 2.0, 2.5, 3.0 and 3.5 bp, respectively.

It is obvious that the unwinding kinetics of RecQ is very different from that of Pif1. The difference is detectable only when the resolution is better than 0.5 bp; even with a 1-bp resolution, one may still not be able to measure the 0.5 bp steps and get only a smeared wide peak in the histogram, hence mistakenly drawing the conclusion that

RecQ unwinds DNA with step sizes of 2-4 bp. Irrespective of the big differences, we show in the following that one can have a general understanding of the stepping kinetics of Pif1, RecQ and, possibly, other helicases. To this end, we argue that (i) a helicase breaks a base pair upon ATP hydrolysis, generating single-stranded nucleotides, 1 nt for each tail of the forked DNA; (ii) unwinding steps, however, are observable only when the generated nucleotides are released; and (iii) in general, it is not necessary that a nucleotide be released concomitantly with its generation because it may stick to some domain of the helicase through, e.g., electrostatic interaction and/or hydrogen bonds [10, 38]. In other words, the helicase may sequester the nascent nucleotides and then release them after a random number of 1-bp opening events (Figure 4). The very general depiction involves three independent parameters, i.e., a base-pair breaking rate  $k_b$ , a 3'-tail releasing rate  $k_{r1}$  and a 5'-tail releasing rate  $k_{r2}$ . The base-pair breaking rate  $k_b$  of a helicase is regulated by the concentration of ATP and can be derived from the unwinding rate versus ATP curve. There is, however, no direct way to calculate the two tail-releasing rates  $k_{r1}$  and  $k_{r2}$ . They can be estimated by using Monte Carlo simulations [40] to reconstruct the histograms of dwell times and step sizes according to the kinetic model sketched in Figure 4.

In our Monte Carlo simulations we made an assumption that the two tail-releasing rates  $k_{r1}$  and  $k_{r2}$  increase with the number of nucleotides sequestered by the helicase. This is necessary because, otherwise, when  $k_b$  became much larger than  $k_{r1}$  and  $k_{r2}$  at high ATP concentrations, the number of nucleotides held by the helicase might become too long to be true. A few physical factors may underlie the assumption. Plausible ones include the reduction of entropy due to confinement of the nucleotides and/or the increase in energy due to accumulation of the negative charges of DNA on the surface of the protein. For simplicity, we assume that the extra energy is proportional to the number of nucleotides held by the helicase. The tail-releasing rates can hence be written as  $k_{ri} = k_{ri}^0 \exp[\alpha(n-1)]$ , where  $i = 1$  or  $2$  and  $k_{ri}^0$  is the rate when  $n = 1$ . Using the values of the breaking rate  $k_b$  from literature [39],  $3.3 \text{ s}^{-1}$  at  $2 \text{ }\mu\text{M}$  ATP and  $6.8 \text{ s}^{-1}$  at  $5 \text{ }\mu\text{M}$  ATP, the reconstructed histograms for RecQ resemble the measured ones when the following parameters are used:  $k_{r1}^0 \approx k_{r2}^0 = 0.3 \text{ s}^{-1}$  and  $\alpha = 0.7$  (Figures. 4b and c). We can also use the Monte Carlo simulation to reconstruct the histograms for Pif1. The nucleotide releasing rates of Pif1 must be, however, at least one order of magnitude higher than the base-pair breaking rate in order to have a good fit. This is equivalent to say that the nucleotides are released immediately after they are generated. As a consequence, the observable unwinding step sizes is 1 bp and the dwell time distributions are exponential with characteristic dwell times depending on the concentration of ATP (Figure 2c). Taken together, the kinetic model sketched in Figure 4 applies to the both helicases with apparently different unwinding behaviors. In addition, a few more simulations with different parameters (data not shown) implied that a histogram of dwell times does not necessarily follow a simple function; it may even not be monotonic under certain conditions.

smFRET has become the technique of choice to study helicases. However, to the best of our knowledge, it has not yet been able to resolve 1-nt step size until now. On one hand, the unprecedented resolution provided by the presented nanotensioner approach enabled us to reveal the details of helicase-catalyzed DNA unwinding that are not easy to study with conventional smFRET method. On the other hand, the high-resolution data also allowed us propose a unified molecular mechanism for the two helicases that belong to two different superfamilies with apparently different unwinding behaviors, implying that many helicases might be more fundamentally correlated.

*Acknowledgements.* This work was supported by a National Science Foundation of China (Grant No. 11674382 (to Y.L.), 11574382 (to M.L.) and 11574381 (to CHX)) and by the Key Research Program of Frontier Sciences, CAS (Grant No. QYZDJ-SSW-SYS014 (to M.L.)).

---

\* Electronic address: yinglu@iphy.ac.cn

† Electronic address: mingli@iphy.ac.cn

- [1] S. S. Patel and K. M. Picha, *Annu. Rev. Biochem.* **69**, 651 (2000).
- [2] S. S. Patel and I. Donmez, *J. Biol. Chem.* **281**, 18265 (2006).
- [3] M. R. Singleton, M. S. Dillingham, and D. B. Wigley, *Annu. Rev. Biochem.* **76**, 23 (2007).
- [4] T. M. Lohman, E. J. Tomko, and C. G. Wu, *Nat. Rev. Mol. Cell Biol.* **9**, 391 (2008).
- [5] J. A. Ali and T. M. Lohman, *Science* **275**, 377 (1997).
- [6] B. Sikora, R. L. Eoff, S. W. Matson, and K. D. Raney, *J. Biol. Chem.* **281**, 36110 (2006).
- [7] R. Ramanagoudr-Bhojappa, S. Chib, A. K. Byrd, S. Aarattuthodiyil, M. Pandey, S. S. Patel, and K. D. Raney, *J. Biol. Chem.* **288**, 16185 (2013).
- [8] Z. Qi, R. A. Pugh, M. Spies, and Y. R. Chemla, *eLife* **2**, e00334 (2013).
- [9] S. Dumont, W. Cheng, V. Serebrov, R. K. Beran, I. Tinoco, Jr., A. M. Pyle, and C. Bustamante, *Nature* **439**, 105 (2006).
- [10] W. Cheng, S. G. Arunajadai, J. R. Moffitt, I. Tinoco, Jr., and C. Bustamante, *Science* **333**, 1746 (2011).
- [11] T. Ha, I. Rasnik, W. Cheng, H. P. Babcock, G. H. Gauss, T. M. Lohman, and S. Chu, *Nature* **419**, 638 (2002).
- [12] S. Syed, M. Pandey, S. S. Patel, and T. Ha, *Cell Rep.* **6**, 1037 (2014).
- [13] S. Myong, M. M. Bruno, A. M. Pyle, and T. Ha, *Science* **317**, 513 (2007).
- [14] G. Lee, M. A. Bratkowski, F. Ding, A. L. Ke, and T. Ha, *Science* **336**, 1726 (2012).
- [15] M. Lee, S. H. Kim, and S. C. Hong, *Proc. Natl. Acad. Sci. U. S. A.* **107**, 4985 (2010).
- [16] X. Long, J. W. Parks, C. R. Bagshaw, and M. D. Stone, *Nucleic Acids Res.* **41**, 2746 (2013).
- [17] F. E. Kemmerich, M. Swoboda, D. J. Kauert, M. S. Grieb, S. Hahn, F. W. Schwarz, R. Seidel, and M. Schlierf, *Nano Lett.* **16**, 381 (2016).
- [18] M. J. Comstock, K. D. Whitley, H. Jia, J. Sokoloski, T. M. Lohman, T. Ha, and Y. R. Chemla, *Science* **348**, 352 (2015).
- [19] E. T. Graves, C. Duboc, J. Fan, F. Stransky, M. Leroux-Coyau, and T. R. Strick, *Nat. Struct. Mol. Biol.* **22**, 452 (2015).
- [20] J. B. Bessler, J. Z. Torres, and V. A. Zakian, *Trends Cell Biol.* **11**, 60 (2001).
- [21] M. L. Bochman, N. Sabouri, and V. A. Zakian, *DNA repair* **9**, 237 (2010).
- [22] J. H. Li et al., *Nucleic Acids Res.* **44**, 4330 (2016).
- [23] V. P. Schulz and V. A. Zakian, *Cell* **76**, 145 (1994).
- [24] J. Zhou, E. K. Monson, S. C. Teng, V. P. Schulz, and V. A. Zakian, *Science* **289**, 771 (2000).
- [25] S. Makovets and E. H. Blackburn, *Nat. Cell Biol.* **11**, 1383 (2009).
- [26] K. Paeschke, J. A. Capra, and V. A. Zakian, *Cell* **145**, 678 (2011).
- [27] P. Janscak, P. L. Garcia, F. Hamburger, Y. Makuta, K. Shiraishi, Y. Imai, H. Ikeda, and T. A. Bickle, *J. Mol. Biol.* **330**, 29 (2003).
- [28] D. A. Bernstein and J. L. Keck, *Nucleic Acids Res.* **31**, 2778 (2003).
- [29] M. E. Fairman-Williams, U. P. Guenther, and E. Jankowsky, *Curr. Opin. Struct. Biol.* **20**, 313 (2010).
- [30] H. Q. Xu, E. Deprez, A. H. Zhang, P. Tauc, M. M. Ladjimi, J. C. Brochon, C. Auclair, and X. G. Xi, *J. Biol. Chem.* **278**, 34925 (2003).

- [31] W. K. Chu and I. D. Hickson, *Nat. Rev. Cancer* **9**, 644 (2009).
- [32] L. Bjergbaek, J. A. Cobb, and S. M. Gasser, *Swiss Med. Wkly* **132**, 433 (2002).
- [33] J. A. Cobb, L. Bjergbaek, and S. M. Gasser, *FEBS Lett.* **529**, 43 (2002).
- [34] C. Bustamante, J. F. Marko, E. D. Siggia, and S. Smith, *Science* **265**, 1599 (1994).
- [35] B. Choi, G. Zocchi, S. Canale, Y. Wu, S. Chan, and L.J. Perry, *Phys. Rev. Lett.* **94**, 038103 (2005).
- [36] B. T. Harada, W. L. Hwang, S. Deindl, N. Chatterjee, B. Bartholomew, and X. Zhuang, *eLife* **5**, e10051 (2016).
- [37] T. R. Blosser, J. G. Yang, M. D. Stone, G. J. Narlikar, and X. Zhuang, *Nature* **462**, 1022 (2009).
- [38] J. A. Newman et al., *Nucleic Acids Res.* **43**, 5221 (2015).
- [39] D. Klaue, D. Kobbe, F. Kemmerich, A. Kozikowska, H. Puchta, and R. Seidel, *Nature communications* **4**, 2024 (2013).
- [40] We consider a process in which the base pair opening and nucleotide releasing events occur independently of each other. At first, a series of time points,  $t_m = m \times \Delta t$ ,  $m=1,2,3, \dots, N$  ( $N > 100,000$ ), at which the base-pair opening may occur, were created by checking at each point a random number  $P$  which is uniformly distributed in the range  $(0, 1)$ . A base-pair opening event occurs if  $P \leq \Delta t \times k_b$ . Secondly, each point in the opening series created above was checked once more. If a newly generated random number  $P$  does not satisfy  $P \leq \Delta t \times k_{r1}$ , then the next point was checked until the inequality is satisfied so that a 3' -tail releasing event occurs. This process is repeated till the end of the base-pair opening series. The interval  $n$  during which no releasing occurs is the step size. In this way, we obtained a series of steps for the releasing of 3' -tail. Repeating the second procedure with  $k_{r2}$ , we got another series of steps for the 5' -tail releasing. After combining the two series of releasing events, the dwell time before each step for both 3' - and 5' -tail was recorded. Finally, the histograms of both step sizes and dwell times were built to compare with the experimental data.

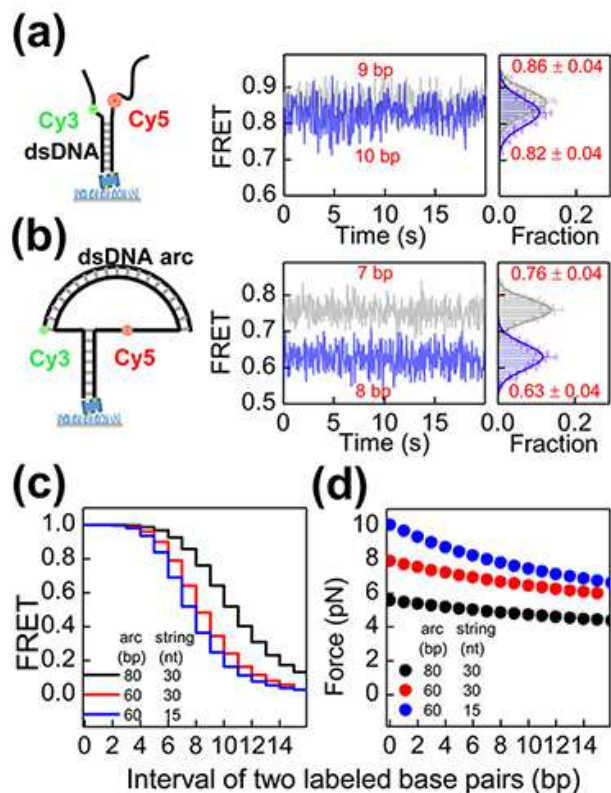


FIG. 1: (Color online). Design of DNA nanotensioners. (a) Free overhangs of a forked DNA fluctuate to blur the FRET signals. The mean FRET efficiency decreases by 0.04 when the Cy3-Cy5 pair is moved from the 9<sup>th</sup> to the 10<sup>th</sup> nucleotide away from the fork. (b) In a nanotensioner, the two ends of a short dsDNA are connected to two ssDNA overhangs of a forked DNA. The dsDNA is bent to exert a force on the fork. The mean FRET efficiency decreases by 0.13 when the Cy3-Cy5 pair is moved from the 7<sup>th</sup> to the 8<sup>th</sup> nucleotide. (c, d) Calculated FRET efficiency (c) and tension (d) as a function of base pairs unwound for various nanotensioners.

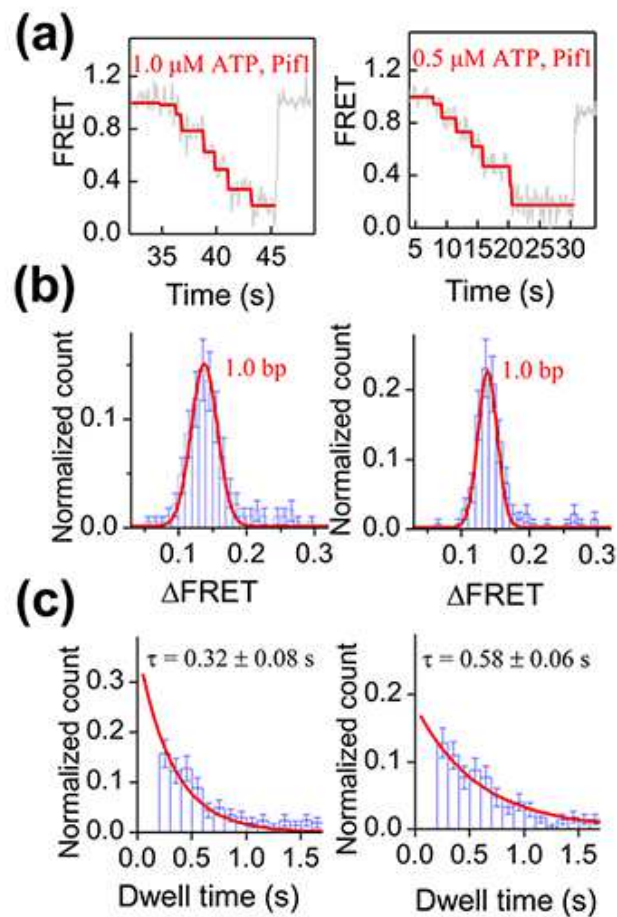


FIG. 2: (Color online). Pif1 unwinds 1 bp at a time in the assay with nanotensioner. (a) Typical FRET traces. (b) Histogram of FRET jumps ( $\Delta\text{FRET}$ ). The red lines represent Gaussian fittings. (c) Histogram of dwell times before each stepping event. The red lines represent single-exponential fittings. The statistics are from  $> 150$  traces at each ATP. The error bars denote SD. The errors in the fits are SEM.

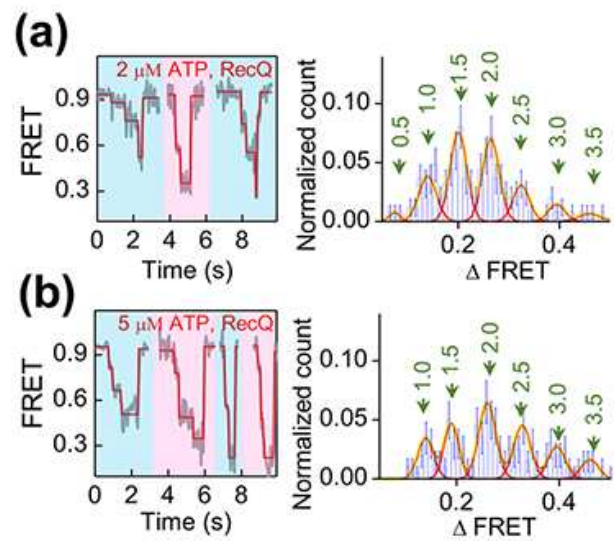


FIG. 3: (Color online). Non-uniform stepwise unwinding by RecQ in the assay with nanotensioner. (a) Typical FRET traces and the corresponding distribution of FRET jumps ( $\Delta$ FRET) at 2  $\mu$ M ATP. (b) Similar data recorded at 5  $\mu$ M ATP. The individual traces are shifted horizontally for clarity. The red lines in the histogram represent Gaussian fittings. The step sizes converted from the FRET jumps are indicated on tops of the peaks. The data are from  $> 200$  traces at each ATP. The error bars denote SD.

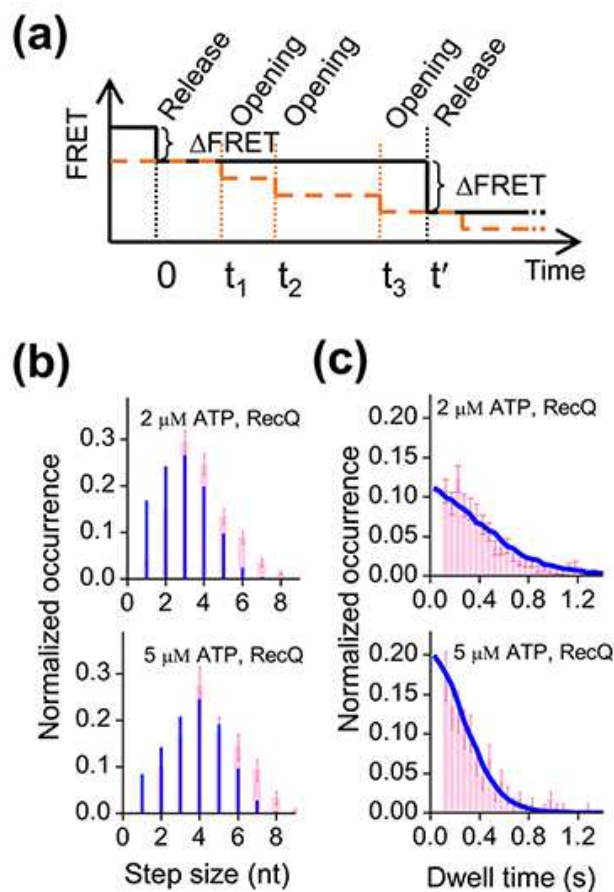


FIG. 4: (Color online). Stepping kinetics of helicase-catalyzed DNA unwinding. (a) Schematic time course of observable FRET signal (black line). At  $t = 0$  and  $t'$ , FRET jumps appear because of the release of the sequestered nascent nucleotides on the 3'- or 5'-strand. The orange dashed line represents the expected time course of the FRET signal if nucleotide release is synchronous with base pair opening, as for Pif1. In the time duration from  $t = 0$  to  $t'$ , base pair opening occurs three times at  $t_1$ ,  $t_2$  and  $t_3$ , respectively. (b, c) Comparison between the Monte Carlo simulated (blue) and the experimentally measured (pink) probabilities of step sizes and dwell times of RecQ. The experimental probabilities in b are peak values in the histograms in Figure 3.